Bacterial Lipopolysaccharide Enhances PDGF Signaling and Pulmonary Fibrosis in Rats Exposed to Carbon Nanotubes

Mark F. Cesta[1,2,3], Jessica P. Ryman-Rasmussen[1,2], Duncan G. Wallace[2], Tiwanda Masinde[3], Geoffrey Hurlburt[4], Alexia J. Taylor[1], and James C. Bonner[1,2]

[1]Department of Environmental and Molecular Toxicology, North Carolina State University, Raleigh, North Carolina; [2]The Hamner Institutes for Health Sciences, Research Triangle Park, North Carolina; [3]Cellular and Molecular Pathology Branch, National Institute of Environmental Health Sciences, Research Triangle Park, North Carolina; and [4]Charles River Laboratories, Pathology Associates, Durham, North Carolina

Engineered multi-walled carbon nanotubes (MWCNT) represent a possible health risk for pulmonary fibrosis due to their fiber-like shape and potential for persistence in the lung. We postulated that bacterial lipopolysaccharide (LPS), a ubiquitous agent in the environment that causes lung inflammation, would enhance fibrosis caused by MWCNT. Rats were exposed to LPS and then intratracheally instilled with MWCNT or carbon black (CB) nanoparticles 24 hours later. Pulmonary fibrosis was observed 21 days after MWCNT exposure, but not with CB. LPS alone caused no fibrosis but enhanced MWCNT-induced fibrosis. LPS plus CB did not significantly increase fibrosis. MWCNT increased platelet-derived growth factor-AA (PDGF-AA), a major mediator of fibrosis. PDGF-AA production in response to MWCNT, but not CB, was synergistically enhanced by LPS. Immunostaining showed PDGF-AA in bronchiolar epithelial cells and macrophages. Since macrophages engulfed MWCNT, were positive for PDGF-AA, and mediate fibroblast responses, experiments were performed with rat lung macrophages (NR8383 cells) and rat lung fibroblasts *in vitro*. LPS exposure increased PDGF-A mRNA levels in NR8383 cells and enhanced MWCNT-induced PDGF-A mRNA levels. Moreover, LPS increased MWCNT- or CB-induced PDGF receptor-α (PDGF-Rα) mRNA in fibroblasts. Our data suggest that LPS exacerbates MWCNT-induced lung fibrosis by amplifying production of PDGF-AA in macrophages and epithelial cells, and by increasing PDGF-Rα on pulmonary fibroblasts. Our findings also suggest that individuals with pre-existing pulmonary inflammation are at greater risk for the potential adverse effects of MWCNT.

Keywords: carbon nanotubes; inflammation; lipopolysaccharide; fibrosis; growth factors

CLINICAL RELEVANCE

The findings reported in this article have important implications for understanding the health risks of inhaled carbon nanotubes. Our research suggests that individuals with pre-existing lung inflammation caused by bacterial lipopolysaccharide are susceptible to pulmonary fibrosis caused by carbon nanotube inhalation exposure.

Carbon nanotubes (CNT) are engineered graphene tubes with unique properties that are anticipated to revolutionize the fields of electronics, structural engineering, and medicine (1–3). The increasing production of single-walled CNT (SWCNT) and multi-walled CNT (MWCNT) is also accompanied by an increase in the potential for human exposure, mainly in occupational settings, but conceivably in the general population as well (4, 5). Unfortunately, some of the physical properties of MWCNT that make them desirable for electronics, engineering, and medicine may augment their toxic potential relative to larger particles or even other types of nanoparticles. Some of these properties include altered surface chemistry compared with larger particles of the same material, a high surface area to volume ratio, a high length to width aspect ratio, and a high degree of biopersistence (4).

A number of studies have addressed the potential of CNTs to cause pulmonary fibrosis, the scarring of lung tissue caused by an increase in fibroblasts and their collagen deposits (6). For example, SWCNT or MWCNT administered by intratracheal instillation or pharyngeal aspiration in mice or rats induce pulmonary granulomas and interstitial lung fibrosis (7–10). Fibrotic reactions in the lungs of mice exposed to SWCNT were associated with increased levels of TGF-β1, a primary mediator of collagen deposition during fibrogenesis (10). We previously reported that SWCNT administered into the lungs of rats by pharyngeal aspiration caused interstitial lung fibrosis that was associated with increased levels of platelet-derived growth factor-AA (PDGF-AA) (11). Most recently we reported increased airway fibrosis and elevated PDGF-AA in the lungs of mice that inhaled MWCNT with ovalbumin allergen challenge (12).

PDGF is a potent mitogen and chemoattractant for fibroblasts and is thought to play a pivotal role in the progression of fibrotic diseases (13). There are four PDGF genes, designated A–D, that encode four homodimeric protein isoforms (PDGF-AA, -BB, -CC, and –DD) and one heterodimeric isoform (PDGF-AB). There are also two PDGF receptors, PDGF-Rα and PDGF-Rβ, that dimerize upon ligand binding, forming three isoforms (PDGF-Rαα, -Rαβ, and -Rββ). PDGF-AA binds exclusively to PDGF-Rα. The cell-surface PDGF-Rα is an inducible receptor that regulates fibroblast mitogenic and chemotactic responses to secreted PDGF after particle or fiber exposure (14). During lung fibrogenesis in rats, PDGF-Rα levels become markedly up-regulated during the fibroblast proliferative stage of the disease (15).

Bacterial lipopolysaccharide (LPS), a component of gram-negative bacterial cell walls, is a potent exogenous inducer of increased fibroblast levels of PDGF-Rα in the lungs of rats (16). LPS is ubiquitous in the environment and has been implicated in a number of occupational lung diseases in humans, most of which are associated with organic dust exposure (17). In experimental animal models, LPS causes airway inflammation with acute exposures and airway remodeling and hyperreactivity with sub-

(*Received in original form March 31, 2009 and in final form July 23, 2009*)

This work was supported by The American Chemistry Council's Long-Range Research Initiative program provided to The Hamner Institutes for Health Sciences, NIH Grant R21-ES015801-01 and NIH Grant RC2 ES018772-01 to J.B.; North Carolina State University's College of Agricultural and Life Sciences; and the Intramural Research Program of the National Institutes of Health, National Institute of Environmental Health Sciences.

Correspondence and requests for reprints should be addressed to James C. Bonner, Ph.D., P.O. Box 7633, NC State University, Raleigh, NC 27695-7633. E-mail: james_bonner@ncsu.edu

Am J Respir Cell Mol Biol Vol 43. pp 142–151, 2010
Originally Published in Press as DOI: 10.1165/rcmb.2009-0113OC on September 8, 2009
Internet address: www.atsjournals.org

chronic exposures. The effects of subchronic pulmonary exposure to LPS are similar to chronic bronchitis, and so subchronic treatment of rodents with LPS is used to model this disease (18, 19). The lung levels of a variety of secreted pro-inflammatory mediators or their cognate receptors are increased by LPS through activation of Toll-like receptor-4 (TLR4) (20). For example, LPS stimulates the release of a number of inflammatory mediators from alveolar macrophages, including tumor necrosis factor (TNF)-α, interleukin (IL)-1β, IL-6, and IL-8 (21, 22). LPS also up-regulates the expression of both PDGF-A and PDGF-B genes in alveolar macrophages (22). These studies suggest that LPS could exacerbate pulmonary fibrosis by "priming" pulmonary macrophages and fibroblasts for enhanced production of cytokines, growth factors, and their receptors.

Little is known regarding the pulmonary fibrotic response to CNTs in the context of pre-existing inflammation. This is an important issue since individuals with bronchitis, chronic obstructive pulmonary disease, asthma, or exposure to high levels of environmental LPS could be particularly sensitive to the adverse effects of CNTs. The purpose of this study was to determine whether pre-exposure to LPS would exacerbate the fibrotic response to MWCNT by amplifying expression of the PDGF-AA and PDGF-Rα genes in the lungs of rats.

MATERIALS AND METHODS

Animals

Six- to eight-week-old male, pathogen-free Sprague-Dawley rats were purchased from Charles River Breeding Laboratories (Kingston, NY) and housed in an Association for Assessment and Accreditation of Laboratory Animal Care (AAALAC)-accredited facility that was humidity and temperature controlled. Rats were housed in microisolator cages on Alphadri cellulose bedding and supplied water and cereal-based diet NIH07 (Zeigler Brothers, Gardners, PA) *ad libitum*. The animal studies were approved by The Hamner Institutes for Health Research Institutional Animal Care and Use Committee.

General Experimental Design

Animals were randomly assigned to six treatment groups of five rats each and acclimated for 1 week before exposure. Rats from three of the treatment groups were exposed to 2.5 mg/kg LPS from *Escherichia coli* (Serotype 026:B6; Sigma-Aldrich, St. Louis, MO) by nasal aspiration, and the rats from the other three treatment groups were exposed to Ca^{2+}- and Mg^{2+}-free phosphate-buffered saline (PBS). Twenty-four hours later, rats were exposed to 4 mg/kg of CB or MWCNT by intratracheal instillation. Negative control animals were treated with PBS. Animals were killed at 1 and 20 days after particle exposure. The lungs were lavaged with PBS and the right lung lobes were minced and placed in RNALater solution (Qiagen, Valencia, CA). Lungs were stored at −20°C and used for RNA isolation. The left lung lobe was collected for histopathology.

Characterization of Bulk CNT

MWCNT were purchased from Helix Material Solutions, Inc. (Richardson, TX). These MWCNT were synthesized by carbon vapor deposition (CVD) with nickel and lanthanum catalysts. Characterization of the size, purity, surface area, and elemental composition of the MWCNT provided by the manufacturer and verified by independent analysis (Millennium Research Laboratories, Inc., Woburn, MA) have been previously reported by our laboratory (12). Size was characterized by transmission electron microscopy (TEM), purity was determined by thermogravimetric analysis (TGA), elemental analysis was performed by energy dispersive X-ray analysis (EDX) and inductively coupled plasma auger electron spectroscopy (ICP-AES), and the specific surface area was determined by BET analysis.

Assay for LPS Contamination

Endotoxin (LPS) was measured by a *Limulus* amebocyte lysate (LAL) assay kit according to manufacturer's specifications (Associates of Cape Cod, East Falmouth, MA). MWCNT were sonicated in vehicle (0.1% Pluronic surfactant in PBS) for 60 minutes at room temperature before performing LAL. The maximum sensitivity of this assay is 0.005 EU/ml. MWCNT suspensions were negative for endotoxin within this detection limit.

Preparation and Instillation of LPS and Nanoparticles

Rats were administered *E. coli* LPS by intranasal aspiration and particles by intratracheal instillation. In brief, animals were anesthetized with isoflurane and approximately 50 μl volume LPS (dose concentration equivalent of 2.5 mg of LPS per kg of bodyweight) or PBS (for control animals) was pipetted into the antrum of the nasal cavity. Twenty-four hours later, the animals were again anesthetized with isoflurane and approximately 100 μl volume of either CB or MWCNT (dose concentration equivalent of 4 mg of particles per kg of body weight) was instilled into the trachea using an 18-gauge catheter attached to a 1.0-ml syringe. The MWCNT suspensions were prepared by first milling the dry particles in a Retsch Mixer Mill (Retsch, Inc., Newtown, PA) for 5 minutes at 30 cycles per second. Just before instillation, the milled nanoparticles were suspended in 1% Pluronic F68 (BASF Corp., Florham Park, NJ), a biocompatible, nonionic surfactant, in PBS and wet milled for an additional 5 minutes, then further diluted with PBS to achieve the desired final dosing concentration suspended in 0.1% Pluronic F68. Carbon black (CB) nanoparticles (Raven 5000 Ultra II) were obtained from Columbian Chemicals Co. (Marietta, GA) and treated in an identical manner to MWCNT for all experiments. All particles were sterilized before instillation. Control rats were administered PBS with 0.1% Pluronic F68 surfactant (vehicle).

Bronchoalveolar Lavage

Rats were killed by pentobarbital overdose and exsanguination via the abdominal aorta, and lungs were lavaged three times with 5-ml volumes of PBS. Bronchoalveolar lavage fluid (BALF) collected from the second and third lavages was pooled (the fluid from the first lavage was kept separate) and all BALF was placed on ice. BAL cells collected by centrifugation were resuspended in culture medium and enumerated using an automated cell counter (Model ZM; Coulter, Marietta, GA). Cytospins were prepared with 25,000 cells per slide. Differential cell counts were performed on HEMA-3 (Fisher Scientific, Pittsburgh, PA)–stained cytocentrifuge slide preparations. Cell numbers were quantified by light microscopy using the ×40 objective, and 500 cells per animal were counted. Total protein and LDH in cell-free BALF from the first two pooled lavages were analyzed spectrophotometrically using a COBAS FARA II (Roche Diagnostic Systems, Inc., Montclair, NJ) and assay kits for LDH (LD Liquid Reagent; Pointe Scientific, Canton, MI) and total protein (Coomassie Plus Protein Assay Reagent; Thermo Scientific, Rockford, IL).

Lung Fixation and Histopathology

One hour before they were killed, rats received a single intraperitoneal injection of 50 mg/kg body weight of bromodeoxyuridine (BrdU; Sigma-Aldrich). At necropsy, the left lungs were pressure-infused intratracheally at 30 cm H_2O with 10% neutral-buffered formalin. Lungs were fixed for approximately 48 hours and then transferred to 70% ethanol. Three cross-sectional portions of the left lung were embedded in paraffin, sectioned at 5 μm, and stained with hematoxylin and eosin (H&E), Masson's trichrome, or immunostained for BrdU by established methods.

Pathology Scoring of Lungs

Three sections of lung (one each from the cranial, middle, and caudal portions of the left lung lobe) from each rat were evaluated in a blinded fashion. Those from the 24-hour time point were scored for inflammation and those from the 21-day time point for inflammation and fibrosis. The inflammation scores reflect the averages of the scores for the number of polymorphonuclear cells, the number and size of intra-alveolar macrophage aggregates (these macrophages were typically laden with nanoparticles), and alveolar wall thickening. Only the lungs from the 21-day time point were scored for fibrosis. The lungs were scored for the amount of collagen present (based on Masson's trichrome-stained sections), the thickness of the

alveolar walls, and the number of fibroblast-like cells associated with the particle-associated lesions. All scores were relative scores on a scale from 0–4, with zero representing the levels of these parameters in the PBS control group, 1 representing minimal change, 2 representing mild change, 3 representing moderate change, and 4 representing marked change.

Immunohistochemistry for PDGF-A

Formalin-fixed, paraffin-embedded rat tissue sections were deparaffinized in xylene and rehydrated through graded ethanols. Endogenous peroxidase was blocked with 3% hydrogen peroxide. Antigen retrieval was performed with the Decloaker pressure cooker and 6.0 M citrate buffer (Biocare Medical, Concord, CA). Protein blocking was performed with 10% normal donkey serum (Jackson Immunoresearch Laboratories, Inc., West Grove, PA) for 20 minutes, followed by the Avidin-Biotin Blocking Kit (Vector Laboratories, Burlingame, CA). Primary antibody, PDGF-A (Santa Cruz Biotechnology, Inc., Santa Cruz, CA), was applied at a 1:25 dilution for 60 minutes at room temperature. For negative controls, the primary antibody was replaced with rabbit nonimmune IgG serum diluted to match the antibody protein concentration and applied at 1:25, also. The slides were incubated in donkey anti-rabbit secondary antibody (Jackson Immunoresearch Laboratories) for 30 minutes at a 1:500 dilution. Label incubation was performed for 30 minutes using the Vectastain Standard Elite Kit (Vector Laboratories). Slides were developed with DAB, counterstained with hematoxylin, dehydrated, cleared, and cover-slipped.

In Vitro Experiments with Cultured Lung Macrophages and Fibroblasts

Primary rat lung fibroblasts (RLFs) were isolated from rats by established methods and cryopreserved (11). Thawed cells were grown in Dulbecco's Modified Eagle's Medium supplemented with 10% fetal bovine serum (FBS), 100 units/ml penicillin G, 100 μg/ml streptomycin, and 0.25 μg/ml amphotericin B in a humidified atmosphere with 5% CO_2 at 37°C. NR8383 cells (Cat. No. CRL-2192; ATCC, Manassas, VA) were grown in F-12K nutrient mixture supplemented with 15% FBS, 100 units/ml penicillin G, 100 μg/ml streptomycin, and 0.25 μg/ml amphotericin B in a humidified atmosphere with 5% CO_2 at 37°C. Upon reaching confluence, 1 μg/ml LPS was added to the culture medium. Twenty-four hours later, the LPS/serum-containing medium was replaced with serum-free medium (F-12 nutrient mixture supplemented with 0.25% bovine serum albumin [BSA], 1 ml Insulin/Transferrin/Selenium [Bio-Whittaker, Walkersville, MD], 100 units/ml penicillin G, 100 μg/ml streptomycin, and 0.25 μg/ml amphotericin B) containing 1 μg/ml LPS. Twenty-four hours later, the medium was removed and the cells were rinsed with warm PBS and treated with 10 μg/cm^2 MWCNT or CB in serum-free medium for 1 h. The medium was then removed, the cells rinsed with warm PBS, and the medium was replaced with fresh serum-free medium. After 4 or 24 hours, the cells were collected and stored at −80°C for later RNA isolation using the Qiagen RNeasy Mini kit.

Taqman Real-Time Quantitative RT-PCR

The lungs were removed from the RNALater solution, blotted dry, and homogenized in buffer RLT (from Qiagen RNeasy Mini kit) with 10 μl/ml β-mercaptoethanol added. Total RNA from right anterior lungs or from cultured cell pellets was isolated using the Qiagen RNeasy Mini kit and converted to cDNA with the High Capacity cDNA Archive Kit (Applied Biosystems, Foster City, CA). Thirty nanograms of cDNA was amplified using Taqman Gene Expression Assays specific for β-actin (Rn_00667869), PDGF-A (Rn_00709363), PDGF-C (Rn_00579958), PDGF-Rα (Rn_01399472), TGF-β1 (Rn_00572010), and Type I procollagen (COL1A2) (Rn_00584426) on the Applied Biosystems 7900 Prism Sequence Detection System. The PCR conditions and data analysis were performed according to the manufacturer's protocol described in User Bulletin No.2, Applied Biosystems Prism 7900 Sequence Detection System. Gene expression was measured by the quantitation of cDNA converted from mRNA corresponding to the target genes relative to the vehicle-treated control groups and normalized to β-actin reference endogenous control. Relative quantitation values ($2^{-\Delta\Delta CT}$) were expressed as fold-change over controls.

Enzyme-Linked Immunosorbent Assays

Quantikine enzyme-linked immunosorbent assay (ELISA) kits (R&D Systems, Minneapolis, MN) were used to assay BALF for total TGF-β1 (active and inactive forms) 24 hours after particle exposure and PDGF-AA 24 hours and 21 days after particle exposure. Duplicate samples using 50 μl BALF were used for each animal. Assays were performed according to kit instructions and absorbances were read on a Multiskan EX microplate spectrophotometer (ThermoFisher Scientific) microplate reader. Values were normalized relative to total protein in BALF and expressed as pg/ml.

Data and Statistical Analysis

All graphs were constructed and statistical analysis performed using GraphPad Prism software v. 5.00 (GraphPad Software, Inc., San Diego, CA). A one-way ANOVA with a *post hoc* Tukey test, Bonferroni test, or Dunnett's test was used to identify significant differences among treatment groups. Significance was set at $P < 0.05$ unless otherwise stated.

RESULTS

Characterization of MWCNT

We have previously reported the physical and chemical properties of the MWCNT used in this study (12). Data from the manufacturer was verified and compared with data from a contracted independent analysis. Residual nickel and lanthinum, catalysts used in the MWCNT manufacturing process, were detected by independent analysis using ICP-AES at 0.34% and 0.03%, respectively. EDX was also used to measure these metals and yielded value of 0.12% for nickel but not detectable levels of lanthanum. MWCNT purity measured by thermogravimetric analysis was greater than 94%, the specific surface area measured by BET analysis was 109 m^2/g, and size ranges of the MWCNT measured by TEM were 10–30 nm width and 0.3–50 μm length. Representative TEM images of the MWCNT along with a typical EDX elemental analysis are shown in Figure 1.

LPS Enhances MWCNT-Induced Pulmonary Interstitial Fibrosis

In this study, LPS was delivered 24 hours before the intratracheal instillation of MWCNT, CB nanoparticle, or vehicle (saline/0.1% Pluronic F68). The lungs of rats receiving intranasal saline then intratracheal saline vehicle, or intranasal LPS then vehicle had no significant lesions at 21 days after exposure (Figures 2A and 2B). MWCNT caused significant fibrosis in the interstitium associated with nanoparticle-induced fibroproliferative lesions in the lungs of rats at 21 days, whereas CB did not (Figures 2C and 2D). These lesions were present in all rats exposed to nanoparticles (CB or MWCNT) with or without LPS and were often present near bronchiolar/alveolar duct junctions, though some appeared to be more distally located. They were more numerous in MWCNT-exposed rats than CB-exposed rats. In rats pre-exposed to LPS, the lesions were larger and more fibrotic. The lesions were characterized by thickening of the alveolar and alveolar duct walls by spindloid cells, macrophages laden with nanoparticles, and extracellular matrix, some of which was identified as collagen upon examination of Masson's trichrome–stained sections. Some of these lesions, particularly in the MWCNT- and MWCNT/LPS-exposed groups, though to a lesser extent in the LPS/CB-exposed rats as well, also exhibited minimal hyperplasia of the epithelium of the terminal bronchioles. Both MWCNT and CB had similar spatial deposition patterns and were localized to the centroacinar region of the lung. Nanoparticles were found both within the cytoplasm of alveolar macrophages and free in the proximal alveolar ducts and adjacent alveoli at 24 hours, and nearly all the

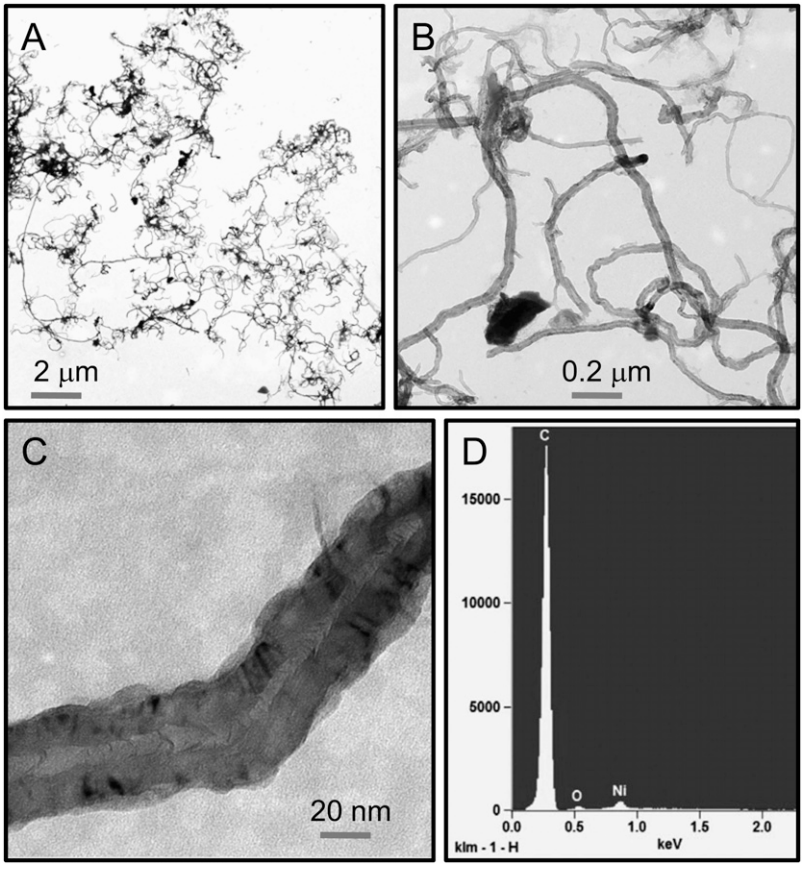

Figure 1. Transmission electron microscopic (TEM) characterization of bulk multi-walled carbon nanotubes (MWCNT). (*A*) Low magnification photomicrograph of MWCNT (*bar* = 2 μm). (*B*) Intermediate magnification TEM image of MWCNT (*bar* = 2 μm). (C) High-magnification TEM photomicrograph of MWCNT (*bar* = 20 nm). (*D*) Energy dispersive X-ray (EDX) analysis of MWCNT.

nanoparticles were found within alveolar macrophages at 21 days. MWCNT or CB exposure, with or without LPS pre-exposure, caused a significant increase in neutrophils retrieved by BAL (Table 1). LPS pre-exposure significantly enhanced interstitial fibrosis associated with MWCNT-induced lesions (Figures 2F and 2H). The combination of LPS and CB caused a mild but not significant fibroproliferative response (Figures 2E and 2G), and CB alone or LPS alone caused no fibrosis. Quantitative pathology scoring showed that only the combination of LPS and MWCNT caused a significant increase in the mean fibrosis score at 21 days after exposure (Figure 3).

LPS Enhances MWCNT-Induced LDH and Total Lung Protein Levels

The level of lactate dehydrogenase (LDH), a marker of cellular injury, in the BALF from the lungs of rats was increased by MWCNT or CB approximately 2-fold compared with vehicle at 24 hours after exposure (Figure 4A). LPS exposure alone did not increase LDH levels compared with vehicle control. However, LPS pre-exposure enhanced MWCNT-induced LDH levels in BALF to a level that was statistically different from vehicle controls. The LDH levels for CB-exposed, CB-exposed/LPS pre-exposed, and MWCNT-exposed rats were elevated compared with controls, but were not statistically different from vehicle controls.

Similar to LDH levels, the total protein level in BALF, a marker of lung injury and inflammation, was increased by MWCNT or CB exposure (Figure 4B). LPS did not increase total protein above vehicle control. MWCNT or CB elevated total protein levels nearly 2-fold above vehicle. LPS pre-exposure enhanced MWCNT-induced total protein to a level that was statistically different from vehicle, but did not enhance CB-induced total protein levels.

LPS Enhances MWCNT-Induced PDGF-AA Secretion in the Lungs of Rats

We next evaluated whether PDGF-AA, a potent chemoattractant and stimulator of fibroblast replication that plays a major role in pulmonary fibrosis, would be elevated in the lungs of rats exposed to MWCNT with or without LPS. PDGF-AA protein levels were measured in BALF samples by ELISA. MWCNT or LPS increased PDGF-AA levels 3- to 4-fold at 24 hours, but levels returned to baseline by 21 days after exposure (Figure 5). LPS pre-exposure synergistically enhanced MWCNT-induced PDGF-AA levels in BAL fluid at 24 hours, but this effect was not observed at 21 days after exposure. In contrast, CB exposure did not increase PDGF-AA levels above control, nor did the combination of LPS and CB increase PDGF-AA. In addition to PDGF-AA, we also measured BALF levels of TGF-β1, which is the key regulator of collagen production during fibrogenesis. TGF-β1 was detectable only in rats pre-exposed to LPS and then exposed to MWCNT, and relatively low levels (5 to 10 pg/ml TGF-β1) were measured (data not shown).

PDGF Immunostaining in the Lungs of Rats Exposed to LPS and MWCNT

Immunohistochemistry was performed using an antibody selective for PDGF-AA. In control animals, PDGF-AA immunoreactivity was most prominent in the airway epithelial cells and alveolar macrophages (Figures 6 and 7). There was less prominent immunostaining in endothelial cells, perivascular cardiac muscle cells, mast cell granules, and some peribronchial and perivascular smooth muscle cells (particularly around larger vessels). In the airways, PDGF-AA immunoreactivity was specific to ciliated epithelial cells; Clara cells, goblet cells, and other nonciliated epithelial cell types were negative. At 1 day after

TABLE 1. DIFFERENTIAL COUNTS OF INFLAMMATORY CELLS IN BRONCHOALVEOLAR LAVAGE FLUID COLLECTED FROM RATS 24 h AFTER EXPOSURE TO MWCNT OR CB NANOPARTICLES, WITH OR WITHOUT A 24-h LPS PRE-EXPOSURE

	Macrophages (% of total cells)	Neutrophils (% of total cells)	Lymphocytes (% of total cells)	Total BAL Cells ($\times 10^3$)
Control	92.44 ± 1.94	4.72 ± 1.23	2.84 ± 0.8	997 ± 58
CB	48.07 ± 1.80*	49.07 ± 1.62*	2.87 ± 0.41	3,210 ± 653
MWCNT	51.33 ± 2.01*	45.87 ± 2.03*	2.80 ± 0.12	1,054 ± 258
LPS	93.25 ± 2.05	4.30 ± 1.88	2.45 ± 0.21	1,729 ± 281
LPS/CB	47.70 ± 0.71*	49.90 ± 1.14*	2.40 ± 0.80	12,906 ± 3,391*
LPS/MWCNT	42.95 ± 4.00†	53.40 ± 4.51†	3.65 ± 0.90	947 ± 173

Definition of abbreviations: BAL, bronchoalveolar lavage; CB, carbon black; LPS, lipopolysaccharide; MWCNT, multi-walled carbon nanotubes.

Data shown are the percent of total cells retrieved from bronchoalveolar lavage along with the total cell number and expressed as the mean ± SE.

* $P < 0.001$ compared to control as determined by one-way ANOVA with post Tukey's test.

† $P < 0.01$ compared to control as determined by one-way ANOVA with post Tukey's test.

exposure, additional PDGF-AA immunostaining was observed in the lungs of rats exposed to the combination of LPS and MWCNT in occasional fibroblast-like cells (elongated, spindle-shaped cells) in thickened alveolar septa and occasional epithelial cells at alveolar duct bifurcations in areas associated with MWCNT-induced inflammation (Figure 6). Similarly, at 21 days after exposure, additional PDGF-AA immunostaining was noted in the hyperplastic epithelium of the terminal bronchioles in animals exposed to MWCNT or to the combination of CB and MWCNT and LPS (Figure 7). Though nanoparticles obscured PDGF-AA immunostaining in many alveolar and interstitial macrophages, positive immunoreactivity could be detected in macrophages that contained fewer nanoparticles. The increased numbers of macrophages in treated groups are the most likely source of increased PDGF-AA, but fibroblasts and airway epithelium, including hyperplastic terminal bronchiolar epithelium, may have contributed to PDGF-AA levels in the lungs of these animals.

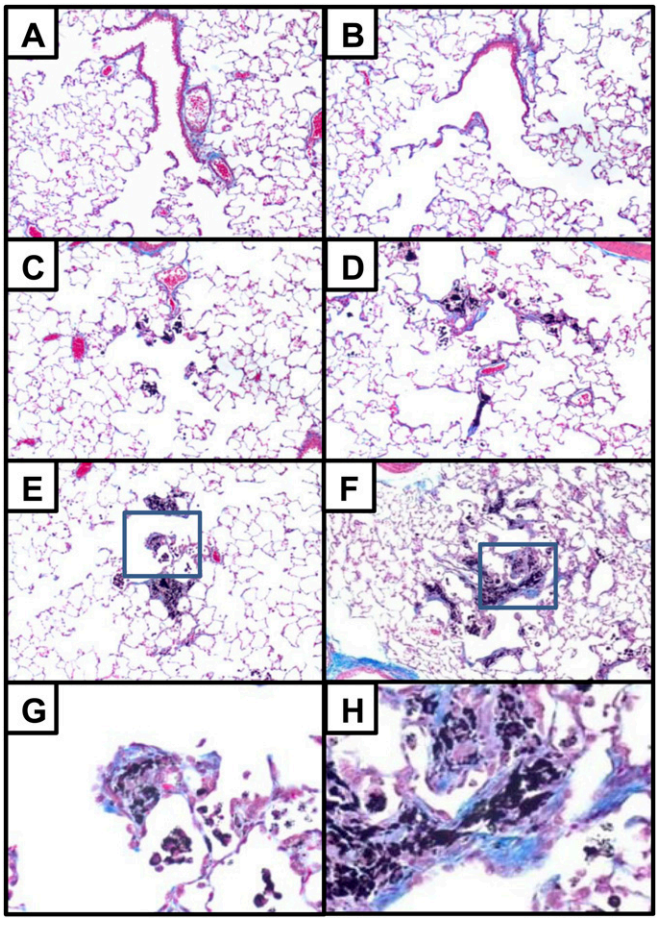

Figure 2. Lung histopathology in rats 21 days after exposure (*blue staining* indicates collagen). (*A*) Saline control. (*B*) Lipopolysaccharide (LPS) alone. (*C*) Carbon black (CB) nanoparticle alone. (*D*) CB nanoparticles with LPS pre-exposure. (*E*) MWCNT alone. (*F*) MWCNT with LPS pre-exposure. (*G*) Higher magnification of *inset* from *E*. (*H*) Higher magnification of *inset* from *F*. *Original magnification*: ×10 for all panels (except *G* and *H*, *original magnification* ×40).

LPS Enhances MWCNT-Induced PDGF-A Chain and PDGF-Rα mRNA Expression in Cultured Lung Macrophages and Fibroblasts *In Vitro*

Since macrophages engulfed the majority of MWCNT in the lung and because they are a major source of PDGF, we investigated the effect of LPS and MWCNT on PDGF and PDGF receptor (PDGF-Rα) mRNA expression levels in a rat lung macrophage cell line (NR8383). Taqman quantitative real-time RT-PCR was used to evaluate mRNA levels for PDGF and PDGF-Rα.

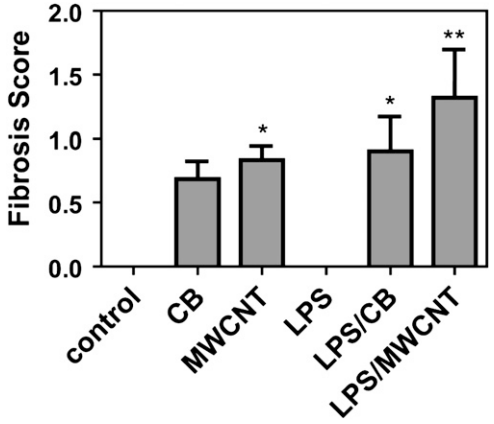

Figure 3. Lung pathology scoring in rats 21 days after exposure. The lungs were scored for the amount of collagen present (based on Masson's trichrome–stained sections), the thickness of the alveolar walls, and the number of fibroblasts associated with the particle-associated lesions. These average scores were then divided by the relative scores for the amount of nanoparticles present in the lungs to give an adjusted average score (*see* MATERIALS AND METHODS). *$P < 0.05$ or **$P < 0.01$ compared with control or LPS as determined by one-way ANOVA with post Dunnett's multiple comparison test.

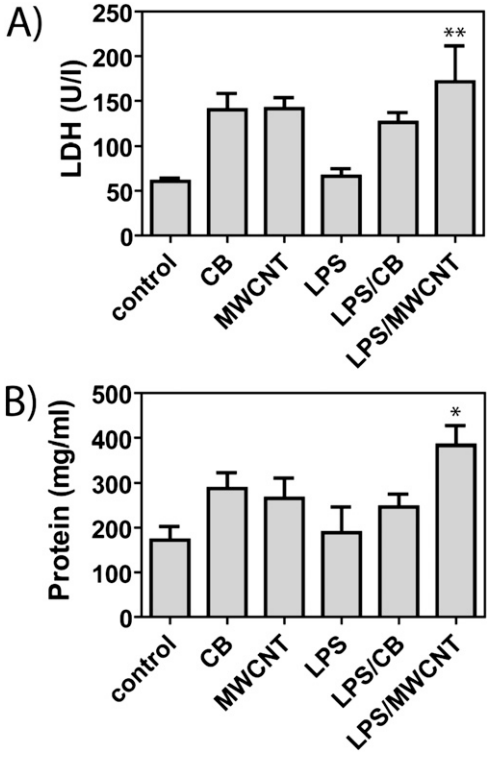

Figure 4. Markers of lung injury. (*A*) Lactate dehydrogenase (LDH) and (*B*) total protein in the lungs of rats 24 hours after exposure to MWCNT or CB nanoparticles, with or without a 24-hour LPS pre-exposure. $*P < 0.05$ or $**P < 0.01$ compared with control or LPS as determined by one-way ANOVA with post Tukey's test or Bonferroni's test.

MWCNT and CB treatment (10 $\mu g/cm^2$) stimulated a marginal, albeit not statistically significant approximately 2-fold increase in PDGF-A and PDGF-Rα mRNA levels in NR8383 macrophages at 4 hours that returned to vehicle control levels by 24 hours (Figures 8A and 8B). LPS alone stimulated 7- to 10-fold increase in PDGF-A mRNA at 4 and 24 hours, and increased PDGF-Rα mRNA approximately 5-fold at 4 hours and returned to control levels by 24 hours. LPS pre-exposure synergistically increased MWCNT or CB-induced PDGF-A and PDGF-Rα mRNA levels (Figures 8A and 8B). We also evaluated the effect of LPS and MWCNT on PDGF and PDGF-Rα mRNA levels in primary passage RLFs, since these cells are the central target cell type that proliferate to PDGF signals and produce collagen during fibrogenesis. MWCNT or CB, with or without LPS, did not affect PDGF-A mRNA levels in RLFs (Figure 9A). MWCNT or CB also did not increase PDGF-Rα mRNA levels in RLFs, but LPS caused a statistically significant increase in PDGF-Rα mRNA, yet this increase was not further increased by MWCNT or CB (Figure 9B).

DISCUSSION

MWCNT have been reported to cause lung fibrosis in mice or rats (9, 23), yet little is known about the effect of pre-existing inflammation on the fibrogenic activity of MWCNT. This is an important issue, since the most susceptible individuals at greatest risk for environmental or occupational exposure to CNT would likely be those with pre-existing respiratory disease. In this study we investigated whether pre-existing lung inflammation caused by bacterial LPS (i.e., endotoxin), a ubiquitous environmental contaminant, would enhance interstitial lung fibrosis caused by

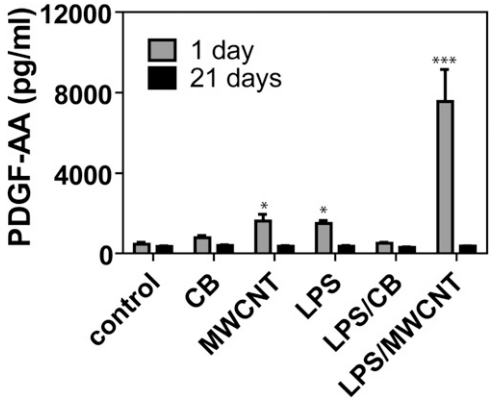

Figure 5. PDGF-AA protein levels in bronchoalveolar lavage (BAL) fluid collected from rats 1 day or 21 days after exposure to 4 mg/kg MWCNT or CB nanoparticles, with or without a 24-hour LPS pre-exposure. PDGF-AA was measured by ELISA. $*P < 0.05$ or $***P < 0.001$ compared with control as determined by one-way ANOVA with post Tukey's test or Bonferroni's test.

MWCNT exposure. LPS pre-exposure enhanced MWCNT-induced lung fibrosis, increased MWCNT-induced lung injury as measured by LDH release and total protein levels, and synergistically elevated MWCNT-induced production of PDGF-AA, a central mediator of fibrosis (13). Therefore, the data presented here support our hypothesis that pre-existing respiratory inflammation resulting from LPS pre-exposure exacerbates the lung fibrotic response to CNT.

LPS is a well-established stimulus of the lung inflammatory response and promotes acute inflammation characterized by the infiltration of circulating neutrophils into the lung, which play a critical role the development of LPS-induced airway disease in chronic exposures (19, 24). In the current study, we did not see an increase in PMNs in the BAL fluid of rats 48 hours after exposure to LPS alone, though there was a slight increase in the total cell numbers. This can be attributed to the short duration of the effects of a single exposure to LPS, which have been shown to resolve completely within 48 hours of exposure (25). Many environmental and occupational lung diseases are caused by LPS that adheres to inhaled particles or fibers. For example, grain dust and cotton worker's lung disease are largely attributed to LPS (26). Also, many ambient air pollution particles cause lung inflammation due to the presence of LPS, which contributes to a complex mixture of organic and inorganic components that comprise these particles (15, 27). Pristine CNT contain little to no LPS, since they are synthesized at very high temperatures. We were unable to detect LPS in our nanotube stock by a commercially available endotoxin assay, but the possibility exists that MWCNT could become contaminated with LPS after the manufacturing process depending upon storage and use conditions. This is because LPS is nearly ubiquitous in the environment and therefore is a common factor that could exacerbate respiratory challenges from other inhaled substances.

The mechanism whereby LPS exacerbates the lung fibrotic response to CNT is not yet known, but our findings suggest that amplification of PDGF-AA and its receptor could play a role in this interactive process. It is well-established that LPS mediates pro-inflammatory effects by binding and activating the transmembrane TLR4, which then signals intracellular signaling pathways that culminate in the production of cytokines such as TNF-α and IL-1, -6, and -8 (28). In addition, LPS docking to the cell surface and coordinated binding to TLR4 is facilitated by the membrane CD14 receptor. We previously reported that LPS, acting through a CD14-dependent mechanism, increased the

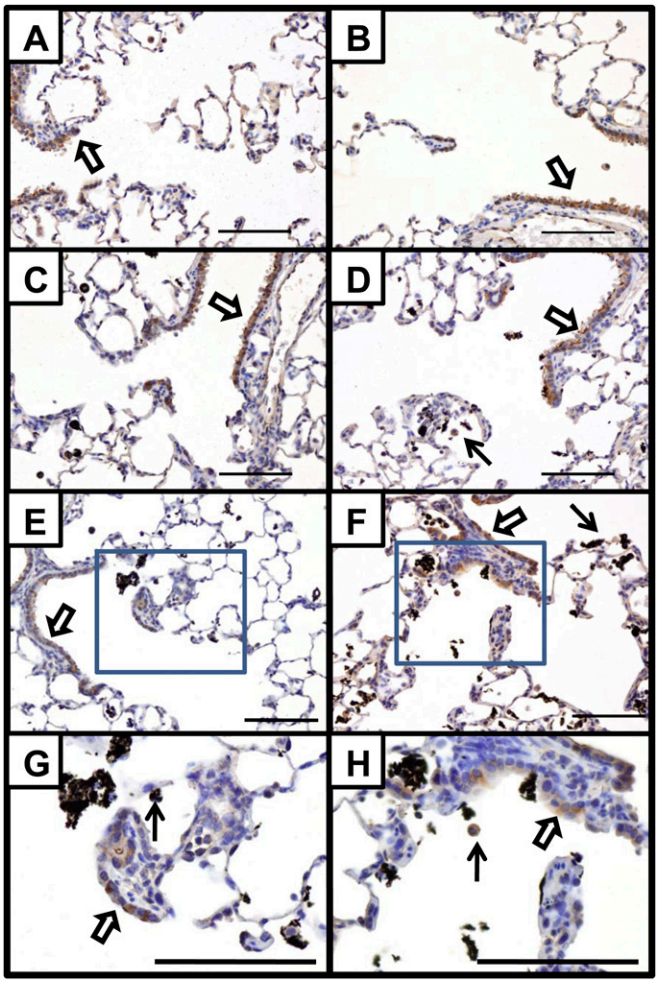

Figure 6. Immunohistochemistry for PDGF-AA at 24 hours after exposure. *Brown staining* indicates PDGF-AA protein. *Open arrows* indicate PDGF-positive epithelium. *Solid arrows* indicate PDGF-positive macrophages, some containing CB or MWCNT. (*A*) Saline control. (*B*) LPS alone. (*C*) CB nanoparticle alone. (*D*) CB nanoparticles with LPS pre-exposure. (*E*) MWCNT alone. (*F*) MWCNT with LPS pre-exposure. (*G*) Higher magnification of *inset* from *E*. (*H*) Higher magnification of *inset* from *F*. Hematoxylin counterstain (*light blue*). *Original magnification*: ×20 for all panels (except *G* and *H*, *original magnification* ×40). *Bars* = 100 μm.

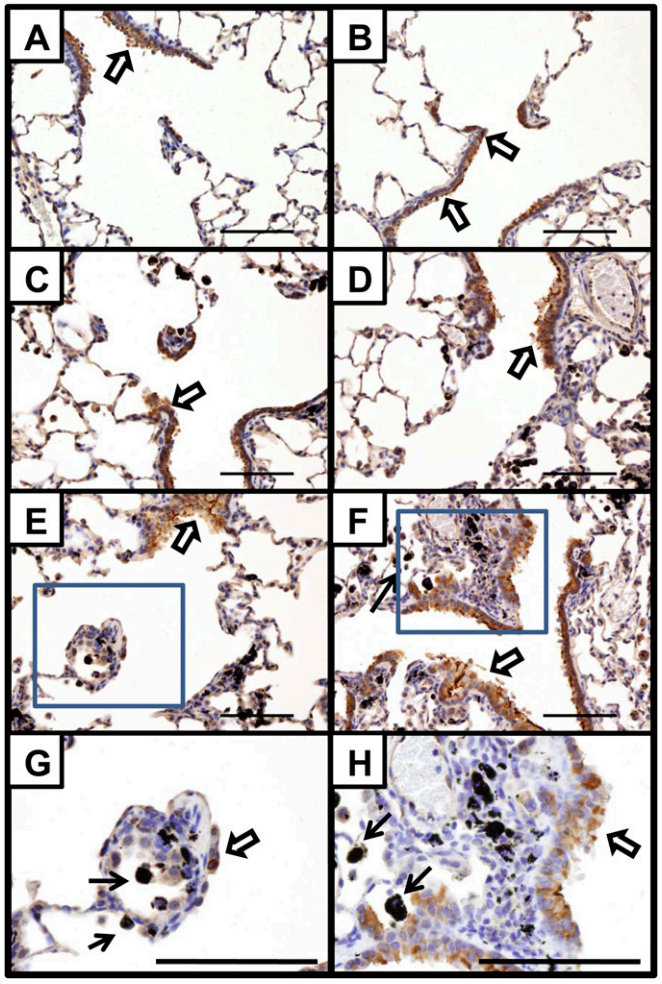

Figure 7. Immunohistochemistry for PDGF-AA at 21 days after exposure. *Brown staining* indicates PDGF-AA protein. *Open arrows* indicate PDGF-positive epithelium. *Solid arrows* indicate PDGF-positive macrophages, some containing CB or MWCNT. (*A*) Saline control. (*B*) LPS alone. (*C*) CB nanoparticle alone. (*D*) CB nanoparticles with LPS pre-exposure. (*E*) MWCNT alone. (*F*) MWCNT with LPS pre-exposure. (*G*) Higher magnification of *inset* from *E*. (*H*) Higher magnification of *inset* from *F*. Hematoxylin counterstain (*light blue*). *Original magnification*: ×20 for all panels (except *G* and *H*, *original magnification* ×40). *Bars* = 100 μm.

numbers of cell-surface PDGF receptors on rat lung fibroblasts (16). Up-regulation of PDGF receptor levels increases the growth and chemotactic responses of fibroblasts to PDGF-AA secreted by macrophages and other lung cell types (13). In the present study, we found that LPS exposure to the lungs of rats increased PDGF-AA protein levels in BAL fluid at 1 day after exposure, but not at 21 days after exposure. However, we detected PDGF-AA protein by immunohistochemistry at both 1 and 21 days. The reason for our inability to detect an increase in secreted PDGF-AA protein in BAL fluid at 21 days in mice treated with MWCNT and/or LPS is unclear. Since the PDGF-AA detected by immunohistochemistry most likely represents a membrane-tethered form and the PDGF-AA detected in BAL fluid by ELISA most likely represents PDGF-AA that has been cleaved from the cell membrane by proteolytic activity, it is conceivable that at 21 days the amount of the cleaved form was decreased to a level below our detection limits, reflecting a decrease in PDGF-AA activity at 21 days after exposure. We also showed that LPS increased PDGF-Rα mRNA levels in primary rat lung fibroblasts and NR8383 cells, a rat lung macrophage cell line. MWCNT exposure to the lungs of rats *in vivo* or to cultured NR8383 cells *in vitro* weakly stimulated PDGF-AA production, but this effect was synergistically amplified by LPS pre-exposure. Therefore, our data show that LPS could enhance MWCNT-induced lung fibrosis by amplifying MWCNT-induced PDGF-AA production in macrophages and epithelial cells and by increasing PDGF receptor levels on fibroblasts, which respond to macrophage- and epithelial-derived PDGF-AA.

Other investigations have shown that bacteria or bacterial-derived products modify the toxicity of CNT. For example, the pharyngeal aspiration of SWCNT into the lungs of mice followed by bacterial infection with *Listeria monocytogenes* 3 day later amplified lung inflammation and collagen formation, and decreased phagocytosis of bacteria by macrophages and bacterial clearance from the lungs of mice (29). This study suggested that enhanced acute inflammation and pulmonary injury with

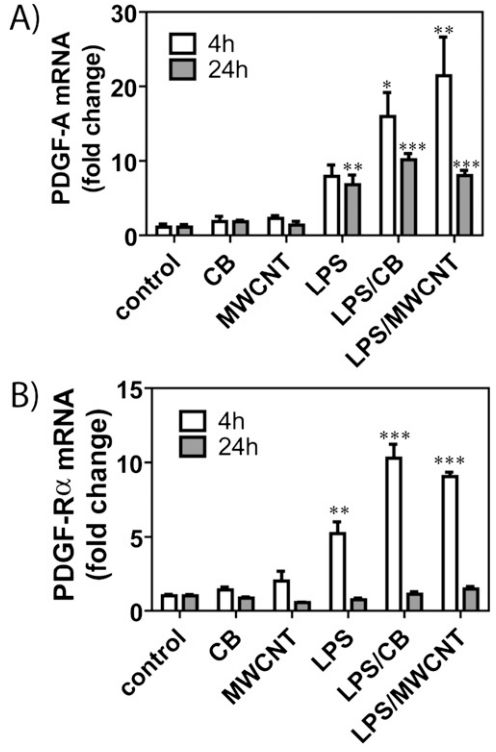

Figure 8. (*A*) PDGF-A and (*B*) PDGF-Rα mRNA levels in rat alveolar macrophages (NR8383 cells) exposed to MWCNT for 4 or 24 hours with or without 1 hour of LPS pre-exposure. Nonadherent cultures of NR8383 cells were grown to near confluence in 10% fetal bovine serum–Dulbecco's Modified Eagle's Medium, then washed and rendered quiescent in serum-free defined medium, and treated with 10 μg/cm^2 MWCNT or CB for 4 or 24 hours before collecting RNA. PDGF-A and PDGF-Rα mRNA levels were measured by real-time RT-PCR as described in MATERIALS AND METHODS. *$P < 0.05$, **$P < 0.01$, or ***$P < 0.001$ compared with control as determined by one-way ANOVA with post Tukey's test or Bonferroni's test.

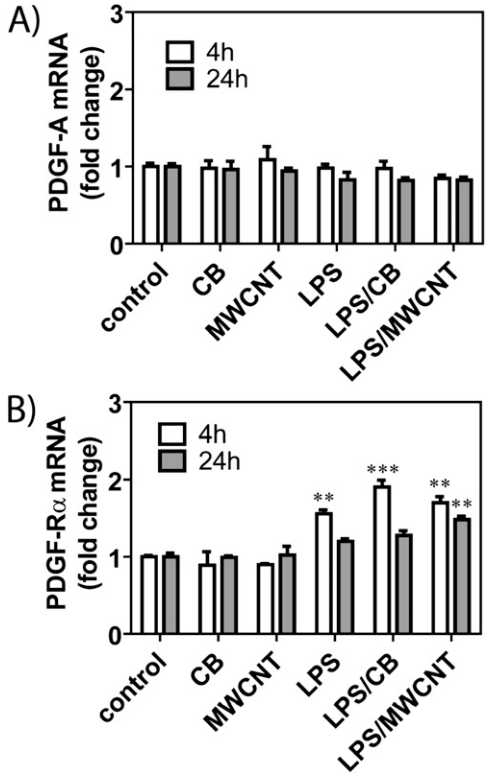

Figure 9. (*A*) PDGF-A and (*B*) PDGF-Rα mRNA levels in early passage rat lung fibroblasts (RLF) exposed to MWCNT for 4 or 24 hours with or without 1 hour of LPS pre-exposure. Confluent, quiescent cultures of RLF were treated with 10 μg/cm^2 MWCNT or CB for 4 or 24 hours before collecting RNA. PDGF-A and PDGF-Rα mRNA levels were measured by Taqman quantitative real-time RT-PCR as described in MATERIALS AND METHODS. **$P < 0.01$, or ***$P < 0.001$ compared with control as determined by one-way ANOVA with post Tukey's test or Bonferroni's test.

delayed bacterial clearance after SWCNT exposure may lead to increased susceptibility to lung infection in exposed populations. In another study, mice that were exposed to SWCNT or MWCNT by intratracheal instillation at the same dose used in our present study (4 mg/kg) developed lung inflammation within 24 hours that was enhanced with LPS co-exposure (30). Moreover, CNT tended to enhance expression of proinflammatory cytokines (TNF-α, IL-1β) in the lung and circulation in the presence of LPS, as well as in cultured mononuclear cells. These results suggested that LPS can facilitate CNT-induced systemic inflammation and possibly affect coagulation, at least in part, via the activation of mononuclear cells.

We recently reported that pre-existing allergic lung inflammation caused by ovalbumin challenge enhanced airway fibrosis in the lungs of C57BL6 mice exposed to MWCNT by inhalation (12). That study also showed that inhaled MWCNT (the same source used in the present study) caused increased production of PDGF-AA in the lungs of mice but MWCNT alone did not cause airway fibrosis. Likewise, ovalbumin allergen challenge alone did not cause airway fibrosis but significantly increased the level of lung TGF-β1. However, the combination of ovalbumin allergen pre-exposure and MWCNT inhalation caused significant airway fibrosis and was accompanied by increases in both PDGF-AA and TGF-β1 (12). These findings support the idea that both PDGF-AA (a stimulator of fibroblast replication) and TGF-β1 (the primary stimulator of fibroblast collagen synthesis) are required and sufficient for airway fibrosis. Moreover, since the mouse ovalbumin model is a well-established model of allergic airway disease, this study suggested that individuals with asthma might be at greater risk for the development of chronic airway disease if exposed to CNT.

The dose and administration methodology used to assess CNT toxicity and to determine the potential of CNT to cause disease are important considerations. Initial studies of CNT on rats and mice used intratracheal instillation or pharyngeal aspiration techniques to deliver a bolus of material to the lung (7–11). The doses administered in these studies ranged from 1 to 4 mg/kg CNT. The dose of 4 mg/kg used in the present study is therefore consistent with these earlier studies. The concern with instillation or aspiration methodologies is that they do not produce deposition patterns similar to inhaled particles (12, 30). However, others have shown that inhalation exposure to SWCNT produce very similar fibrogenic effects to those seen after a pharyngeal exposure route (31). While our methodology in the present studies achieved a well-dispersed dose of MWCNT in the lungs of rats, further study should address the effect LPS pre-exposure on inhaled MWCNT.

Our findings with MWCNT in the absence of LPS in the present study share some similarities and differences to a previous study in which we intratracheally instilled SWCNT into rats (11), which provides a comparison of the pulmonary effects of MWCNT and SWCNT. In our previous study, rats exposed to

SWCNT also developed interstitial fibrotic lesions in the same anatomic regions of the lung (terminal bronchiolar and alveolar regions) and had increased PDGF-AA (11). The fibrotic lesions were relatively diffuse and localized to areas of CNT deposition, and therefore we did not detect a significant increase in total lung collagen content. For this reason, in the present study we did not measure total lung collagen by hydroxyproline or Sircol assay, but instead used a histopathologic scoring method. The trace metal content of MWCNT (nickel and lanthanum) differed from the trace metal content of SWCNT (cobalt and molybdenum). The lengths of both the SWCNT and MWCNT exceeded 10 μm; however, the MWCNT were 30 to 50 nm in width, whereas the SWCNT were 1 to 3 nm in width. Most importantly, SWCNT caused the formation of many unique bridge structures between alveolar macrophages in the lungs of rats (11), whereas no such bridge structures were observed in the lungs of rats that were exposed to MWCNT.

The mechanism through which MWCNT or SWCNT increased PDGF-AA production is unknown. CNT have some features in common with asbestos fibers (e.g., high aspect ratio, residual metals), which are also known to increase PDGF by macrophages and fibroblasts (32, 33). However, metals in asbestos fibers (e.g., iron, magnesium) are naturally occurring, whereas CNT are manufactured using metal catalysts such as iron, nickel, and cobalt. Nickel was a catalyst present in the MWCNT used in the present study, and nickel has been reported to increase PDGF production by human macrophages (34) and cause pulmonary fibrosis in experimental animals and in humans exposed occupationally (35). Therefore, we speculate that the fibrogenic potential of MWCNT is due at least in part to residual nickel catalyst.

In our hands, SWCNT or MWCNT are weak inducers of TGF-β1 production in the lung. Our previous work with SWCNT showed no significant increase in lung TGF-β1 mRNA in rats exposed by pharyngeal aspiration (11). In contrast, other work has shown that SWCNT increased TGF-β1 levels in the lungs of mice (10). TGF-β1 levels in BAL fluid peaked at 7 days after exposure in these mice and then returned to near baseline levels by 28 days after exposure. Therefore, it is possible that in our studies with rats, which were evaluated either 1 or 21 days after exposure to SWCNT (11) or MWCNT in the present study, we simply missed the window of TGF-β1 expression. We did observe low levels of TGF-β1 protein in the BAL fluid from rats exposed to LPS and MWCNT, which indicates that this important stimulator of collagen production is expressed under conditions that result in maximal fibrosis. A caveat is that we measured TGF-β1 by ELISA and such colorimetric assays are prone to some interference of protein binding and/or enzymatic activity by carbonaceous particles. While we were able to measure MWCNT-induced increases in the level of PDGF by ELISA, we cannot rule out some interference of nanoparticles in ELISA assays for measuring growth factor levels.

In summary, we report that pre-exposure to bacterial LPS enhances the fibrogenic effect of MWCNT delivered to the lungs of rats. Exacerbation of MWCNT-induced fibrosis by LPS is accompanied by enhanced production of PDGF-AA and its receptor in the lungs of rats, as well as in cultured rat lung macrophages and fibroblasts. Given the importance of the PDGF system in fibrotic diseases, our data indicate a possible mechanism of action whereby LPS increases MWCNT-induced fibrosis in two ways. First, LPS synergistically elevates macrophage production of PDGF-AA by MWCNT. Second, LPS upregulates the receptor to which PDGF-AA binds on fibroblasts, thereby amplifying growth and chemotactic responses. In general, our data support the hypothesis that pre-existing inflammation exacerbates the fibrogenic response of the lungs to CNT.

Author Disclosure: M.F.C. has received funding from the National Institutes of Health (NIH) (National Institute of Environmental Health Sciences [NIEHS]) ($100,001 or more). J.P.R.-R. is an employee of American Chemistry Council Long Range Research Initiative. D.G.W. is an employee of Gilead Sciences, Inc. T.M. is an employee for the NIEHS. JC.B. has received fees from NIH for consultancies (up to $1,000). None of the other authors has a financial relationship with a commercial entity that has an interest in the subject of this manuscript.

Acknowledgments: The authors thank David Weil, Delorise Williams, Otis Light, Vickie Wong, Elise Barber, and Carol Bobbitt at The Hamner Institutes, Natasha Clayton at NIEHS, and J. Todd Pointer at Integrated Laboratory Systems, Inc. for excellent technical assistance. The authors also thank Greg Parsons and Joe Spagnola at NCSU for helpful comments about MWCNT TEM and SEM data and Ram Bhat at Millennium Research, Inc., for directing contracted MWCNT characterizations. Special thanks to Mel Andersen and Darol Dodd at The Hamner Institutes for helpful comments during the preparation of this manuscript.

References

1. Baughman RH, Zakhidov AA, de Heer WA. Carbon nanotubes – the route toward applications. *Science* 2002;297:787–792.
2. Avouris P, Chen Z, Perebeinos V. Carbon-based electronics. *Nat Nanotechnol* 2007;2:605–615.
3. Bianco A, Kostarelos K, Prato M. Applications of carbon nanotubes in drug delivery. *Curr Opin Chem Biol* 2005;9:674–679.
4. Donaldson K, Aitken R, Tran L, Stone V, Duffin R, Forrest G, Alexander A. Carbon nanotubes: a review of their properties in relation to pulmonary toxicology and workplace safety. *Toxicol Sci* 2006;92:5–22.
5. Card JW, Zeldin DC, Bonner JC, Nestmann ER. Pulmonary applications and toxicity of engineered nanoparticles. *Am J Physiol Lung Cell Mol Physiol* 2008;295:L400–L411.
6. Wynn T. Cellular and molecular mechanisms of fibrosis. *J Pathol* 2008; 214:199–210.
7. Warheit DB, Laurence BR, Reed KL, Roach DH, Reynolds GA, Webb TR. Comparative pulmonary toxicity assessment of single-wall carbon nanotubes in rats. *Toxicol Sci* 2004;77:117–125.
8. Lam CW, James JT, McCluskey R, Hunter RL. Pulmonary toxicity of single-wall carbon nanotubes in mice 7 and 90 days after intratracheal instillation. *Toxicol Sci* 2004;77:126–134.
9. Muller J, Huaux F, Moreau N, Misson P, Heilier JF, Delos M, Arras M, Fonseca A, Nagy JB, Lison D. Respiratory toxicity of multi-wall carbon nanotubes. *Toxicol Appl Pharmacol* 2005;207:221–231.
10. Shvedova AA, Kisin ER, Mercer R, Murray AR, Johnson VJ, Potapovich AI, Tyurina YY, Gorelik O, Arepalli S, Schwegler-Berry D, *et al.* Unusual inflammatory and fibrogenic pulmonary responses to single-walled carbon nanotubes in mice. *Am J Physiol Lung Cell Mol Physiol* 2005;289:L698–L708.
11. Mangum JB, Turpin EA, Antao-Menezes A, Cesta MF, Bermudez E, Bonner JC. Single-walled carbon nanotube (SWCNT)-induced interstitial fibrosis in the lungs of rats is associated with increased levels of PDGF mRNA and the formation of unique intercellular carbon structures that bridge alveolar macrophages in situ. *Part Fibre Toxicol* 2006;3:15.
12. Ryman-Rasmussen JP, Tewksbury EW, Moss OR, Cesta MF, Wong BA, Bonner JC. Inhaled multi-walled carbon nanotubes potentiate airway fibrosis in murine allergic asthma. *Am J Respir Cell Mol Biol* 2009;40: 349–358.
13. Bonner JC. Regulation of PDGF and its receptors in fibrotic diseases. *Cytokine Growth Factor Rev* 2004;15:255–273.
14. Lindroos PM, Coin PG, Badgett A, Morgan DL, Bonner JC. Alveolar macrophages stimulated with titanium dioxide, chrysotile asbestos, and residual oil fly ash upregulate the PDGF receptor-alpha on lung fibroblasts through an IL-1beta-dependent mechanism. *Am J Respir Cell Mol Biol* 1997;16:283–292.
15. Bonner JC, Lindroos PM, Rice AB, Moomaw CR, Morgan DL. Induction of PDGF receptor-alpha in rat myofibroblasts during pulmonary fibrogenesis in vivo. *Am J Physiol Lung Cell Mol Physiol* 1998; 274:L72–L80.
16. Coin PG, Lindroos PM, Bird GS, Osornio-Vargas AR, Roggli VL, Bonner JC. Lipopolysaccharide up-regulates platelet-derived growth factor (PDGF) alpha-receptor expression in rat lung myofibroblasts and enhances response to all PDGF isoforms. *J Immunol* 1996;156:4797–4806.
17. Thorn J. The inflammatory response in humans after inhalation of bacterial endotoxin: a review. *Inflamm Res* 2001;50:254–261.
18. Nikula KJ, Green FH. Animal models of chronic bronchitis and their relevance to studies of particle-induced disease. *Inhal Toxicol* 2000; 12:123–153.

19. Brass DM, Savov JD, Gavett SH, Haykal-Coates N, Schwartz DA. Subchronic endotoxin inhalation causes persistent airway disease. *Am J Physiol* 2003;285:L755–L761.
20. Schroder K, Sweet MJ, Hume DA. Signal integration between IFN-gamma and TLR signalling pathways in macrophages. *Immunobiology* 2006;211:511–524.
21. Becker S, Mundandhara S, Devlin RB, Madden M. Regulation of cytokine production in human alveolar macrophages and airway epithelial cells in response to ambient air pollution particles: Further mechanistic studies. *Toxicol Appl Pharmacol* 2005;207: 269–275.
22. Nagaoka I, Trapnell BC, Crystal RG. Upregulation of platelet-derived growth factor-A and -B gene expression in alveolar macrophages of individuals with idiopathic pulmonary fibrosis. *J Clin Invest* 1990;85: 2023–2027.
23. Li JG, Li WX, Xu JY, Cai XQ, Liu RL, Li YJ, Zhao QF, Li QN. Comparative study of pathological lesions induced by multiwalled carbon nanotubes in lungs of mice by intratracheal instillation and inhalation. *Environ Toxicol* 2007;22:415–421.
24. Savov JD, Gavett SH, Brass DM, Costa DL, Schwartz DA. Neutrophils play a critical role in development of LPS-induced airway disease. *Am J Physiol Lung Cell Mol Physiol* 2002;283:L952–L962.
25. Wohlford-Lenane CL, Deetz DC, Schwartz DA. Cytokine gene expression after inhalation of corn dust. *Am J Physiol* 1999;276:L736–L743.
26. Schwartz DA. Inhaled endotoxin, a risk for airway disease in some people. *Respir Physiol* 2001;128:47–55.
27. Becker S, Fenton MJ, Soukup JM. Involvement of microbial components and toll-like receptors 2 and 4 in cytokine responses to air pollution particles. *Am J Respir Cell Mol Biol* 2002;27:611–618.
28. Lu YC, Yeh WC, Ohashi PS. LPS/TLR4 signal transduction pathway. *Cytokine* 2008;42:145–151.
29. Shvedova AA, Fabisiak JP, Kisin ER, Murray AR, Roberts JR, Tyurina YY, Antonini JM, Feng WH, Kommineni C, Reynolds J, *et al.* Sequential exposure to carbon nanotubes and bacteria enhances pulmonary inflammation and infectivity. *Am J Respir Cell Mol Biol* 2008;38:579–590.
30. Inoue K, Takano H, Koike E, Yanagisawa R, Sakurai M, Tasaka S, Ishizaka A, Shimada A. Effects of pulmonary exposure to carbon nanotubes on lung and systemic inflammation with coagulatory disturbance induced by lipopolysaccharide in mice. *Exp Biol Med* 2008;233:1583–1590.
31. Shvedova AA, Kisin E, Murray AR, Johnson VJ, Gorelik O, Arepalli S, Hubbs AF, Mercer RR, Keohavong P, Sussman N, *et al.* Inhalation vs. aspiration of single-walled carbon nanotubes in C57BL/6 mice: inflammation, fibrosis, oxidative stress, and mutagenesis. *Am J Physiol Lung Cell Mol Physiol* 2008b;295:L552–L565.
32. Lasky JA, Coin PG, Lindroos PM, Ostrowski LE, Brody AR, Bonner JC. Chrysotile asbestos stimulates platelet-derived growth factor-AA production by rat lung fibroblasts *in vitro*: evidence for an autocrine loop. *Am J Respir Cell Mol Biol* 1995;12:162–170.
33. Bonner JC, Osornio-Vargas AR, Badgett A, Brody AR. Differential proliferation of rat lung fibroblasts induced by the platelet-derived growth factor-AA, -AB, and -BB isoforms secreted by rat alveolar macrophages. *Am J Respir Cell Mol Biol* 1991;5:539–547.
34. Kuwabara K, Ogawa S, Matsumoto M, Koga S, Clauss M, Pinsky DJ, Lyn P, Leavy J, Witte L, Joseph-Silverstein J, *et al.* Hypoxia-mediated induction of acidic/basic fibroblast growth factor and platelet-derived growth factor in mononuclear phagocytes stimulates growth of hypoxic endothelial cells. *Proc Natl Acad Sci USA* 1995;92:4606–4610.
35. Kelleher P, Pacheco K, Newman LS. Inorganic dust pneumonias: the metal-related parenchymal disorders. *Environ Health Perspect* 2000; 108:685–696.